

# Fabrication of Microcapsules for Dye-Doped Polymer-Dispersed Liquid Crystal-Based Smart Windows

Mingyun Kim,<sup>†</sup> Kyun Joo Park,<sup>†</sup> Seunghwan Seok,<sup>†</sup> Jong Min Ok,<sup>†</sup> Hee-Tae Jung,<sup>†</sup> Jaehoon Choe,<sup>‡</sup> and Do Hyun Kim<sup>\*,†</sup>

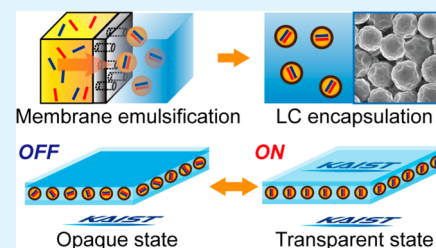
<sup>†</sup>Department of Chemical & Biomolecular Engineering, KAIST, 291, Daehak-ro, Yuseong-gu, Daejeon 305-701, Republic of Korea

<sup>‡</sup>Research Park, LG Chem, 188, Munji-ro, Yuseong-gu, Daejeon 305-738, Republic of Korea

## S Supporting Information

**ABSTRACT:** A dye-doped polymer-dispersed liquid crystal (PDLC) is an attractive material for application in smart windows. Smart windows using a PDLC can be operated simply and have a high contrast ratio compared to those of other devices that employed photochromic or thermochromic material. However, in conventional dye-doped PDLC methods, dye contamination can cause problems and has a limited degree of commercialization of electric smart windows. Here, we report on an approach to resolve dye-related problems by encapsulating the dye in monodispersed capsules. By encapsulation, a fabricated dye-doped PDLC had a contrast ratio of >120 at 600 nm. This fabrication method of encapsulating the dye in a core-shell structured microcapsule in a dye-doped PDLC device provides a practical platform for dye-doped PDLC-based smart windows.

**KEYWORDS:** smart windows, dye-doped PDLC, polymer-dispersed liquid crystal (PDLC), core-shell structure, polyurethane capsule, optical materials



## 1. INTRODUCTION

Electro-optical switchable materials have been studied extensively to develop smart glass or smart windows that function through light transmission changes in response to a simple electric charge.<sup>1–6</sup> For smart windows, polymer-dispersed liquid crystal (PDLC) devices have been studied extensively, which can control the transmission of light by an applied voltage.<sup>7–10</sup> For practical use in smart windows, it is necessary to have a distinct transition between an opaque and transparent state. As such, a high contrast ratio (CR) is critical for an improved switching-state yield.

Until now, high switching yields with chromism have been achieved by using dichroic dyes.<sup>11–14</sup> However, the use of the dichroic dye may cause stain contamination from dye residue inside the polymer matrix. This results in the altered absorption of UV light by the dye, causing poor polymerization of the polymer matrix.<sup>11,12,14–16</sup> These dye-related problems can be responsible for a low switching-state yield, a short lifetime, and a high driving voltage for the operation of a dye-doped PDLC device. Thus, it is important to overcome dye-related problems and enhance the CR in the development of a dye-doped PDLC.

A material encapsulation technique using core-shell structured microcapsules may be a good candidate for manufacturing a dye-doped PDLC. Via the adoption of the encapsulation method, LC with a dye can be isolated in microcapsules, resulting in the separation of dyes from the polymer matrix. Furthermore, monodispersed LC-containing capsules can provide enhanced light transmission by preventing the light scattering caused by differently sized LC droplets.<sup>9,17</sup>

Thus far, the microcapsule fabrication technique has shown tremendous improvements by employing various methods such as a layer-by-layer (LbL) method, microfluidic droplet generation, and membrane emulsification.<sup>18–24</sup> Those methods can open new avenues to overcome the limitations of dye-doped PDLCs, which include dye-related issues and additional light scattering due to LC distribution.

In this study, we fabricated uniform-sized microcapsules with LC/dichroic dye cores and polyurethane/polyurea (PU/PUR) shells to create a dye-doped PDLC with a high CR. To prevent dye-related problems and to increase the CR, we fabricated the LC/dye-encapsulating polyurethane particles through integration of membrane emulsification and interfacial polymerization. Membrane emulsification produced monodispersed LC droplets  $\sim 4.5 \mu\text{m}$  in diameter, and the capsules were directly made through interfacial polymerization on the surface of the liquid core.<sup>25–28</sup> Isolation of LC with the dye by the PU/PUR capsule allowed us to avoid previously reported dye-related issues. Using LC/dye-encapsulated capsules, we demonstrated the switch from transparent and opaque states of a dye-doped PDLC through control of an ac current. We also performed optical evaluations, including light transmittance and CR, to demonstrate its practical application in smart windows.

**Received:** May 23, 2015

**Accepted:** July 20, 2015

**Published:** July 20, 2015

## 2. EXPERIMENTAL SECTION

**2.1. Materials.** Isophorone diisocyanate (IPDI), polypropylene glycol (PPG,  $M_w \sim 2000$ ), diethylenetriamine (DETA), dibutyltin dilaurate (DBTDL), polystyrene (PS) particle (10  $\mu\text{m}$ ), Tween 20, square-shaped indium tin oxide (ITO)-coated glass (surface resistivity of 70–100  $\Omega/\text{sq}$ , refractive index of 1.517), and polyvinylpyrrolidone (PVP,  $M_w \sim 10000$ ) were purchased from Sigma-Aldrich. ABIL EM 90 was purchased from Evonik Industries. LC (HPC 21600-000) and Sudan black B (SBB) were obtained from HCCH China and TCI America, respectively. The nematic–isotropic transition temperature of LC was 95  $^\circ\text{C}$ , and refractive indices of LC are as follows:  $n_o = 1.524$ ,  $n_e = 1.765$  at 589 nm, 20  $^\circ\text{C}$ . NOA 65 was purchased from Norland Products, and the refractive index of the cured polymer was 1.524. Deionized (DI) water (Human UP900, Human Corp.) was used for all aqueous solutions. All chemicals were used as received without purification.

**2.2. Preparation of Emulsions and Microcapsules.** The dispersed phase consisted of 9.385 g of LC, 3.33 g of IPDI (1.0 M), 1.8 g of PPG (0.06 M), 0.45 g of ABIL EM 90 (3 wt %), and 0.01 g of SBB (0.1 wt %).<sup>29</sup> A mixture of 180 mL of DI water, 0.25% PVP (w/v), and 0.0074% Tween 20 (w/v) was used as the continuous phase. In this study, ABIL EM 90, PVP, and Tween 20 were used as a surfactant to stabilize the emulsions and prevent droplet merging. The microdroplets were generated by using a 1.1  $\mu\text{m}$  pore SPG membrane device (IMK-40M1, MC Tech) under a pressure of 20.2 kPa using nitrogen gas. In the reservoir, as a dispersed phase, an LC solution was passed through the membrane and a continuous phase was stirred at 175 rpm. The procedures are schematically shown in Figure S1. To make a PU/PUR shell, the generated emulsion was first mixed with 0.03 g of DBTDL in a beaker and then mixed with the aqueous solution of DETA (30.9 g), Tween 20 (0.07 g), PVP (0.3 g), and DI water (90 mL) at 60  $^\circ\text{C}$ . Then, the beaker was sealed, and the solution was stirred gently at 60  $^\circ\text{C}$  for 5 h. To characterize the generation of the capsule quantitatively, the yield was defined as the weight ratio between products and reactants. The obtained capsules were 13 g on average using the conditions described here. According to the number of functional groups in IPDI (two groups) and DETA (three groups), supposing IPDI and DETA reacted with a 1.5:1 ratio, 1.03 g of DETA reacted with 3.33 g of IPDI in the dispersed phase. Thus, the yield was 81%.

**2.3. Stability Test of Capsules.** To confirm the LC/dye protection performance of the capsules, we dispersed the LC/dye-containing capsules, cracked capsules using a mortar, and naked droplets. Each sample (1 g) was dispersed in DI water (30 mL) for 1 h. Then, 1 mL of the solution was obtained, and samples were separated with a centrifuge. The separated water was analyzed with a Fourier transform infrared spectroscopy microscope (FT-IR, ALPHA, BRUKER). In addition, we dispersed the capsules (0.03 g) in DI water (12 mL) to confirm the stability of capsules depending on time. After mixing, 1 mL of the solution was obtained, and the capsules were separated with a centrifuge. The separated water was analyzed by FT-IR.

**2.4. Fabrication of a Dye-Doped PDLC Device.** To fabricate a dye-doped PDLC device, LC-encapsulating microcapsules, uncured NOA 65, 10  $\mu\text{m}$  diameter PS particle spacers for a uniform thickness, and two ITO glasses were used. For the uniform dispersion of LC capsules, 0.1 g of PS particles and 0.3 g of LC capsules were mixed in 1 g of DI water. Then, ITO glass was coated with 0.05 g of LC capsules and the PS mixture. After being coated, the glass was dried at room temperature for 12 h to evaporate the water completely. To make a polymer matrix, 0.025 g of NOA 65 was coated on the other ITO glass. Then, two ITO glasses were assembled together so that the glasses were stacked with each other and pressed. Finally, NOA 65 was cured by applying 7.5  $\text{J}/\text{cm}^2$  of UV irradiation at 365 nm.

**2.5. Electro-optical Property Measurements.** The electro-optical property of the dye-doped PDLC was measured by applied voltage in the range of 0–100 V for a dye-doped PDLC device at 1 kHz using a function generator (33220A, Agilent/HP), a voltage amplifier (F10A, FLC Electronics), and UV–vis spectroscopy

(OPTIZEN 3220UV, MECASYS). The function generator can apply 0–10 V in 1 kHz, and the voltage amplifier can amplify the voltage 10 times. UV–vis spectroscopy was used to monitor the transmittance change of the dye-doped PDLC device according to the applied voltage.

**2.6. Instruments.** A field-emission transmission electron microscope (FE-TEM, Tecnai TF30 ST, FEI Co.), a field-emission scanning electron microscope (FE-SEM, S-4800, Hitachi), and a polarized optical microscope (POM, LV-100POL, Nikon) with a charge-coupled device (CCD) camera were used to characterize the morphology of the capsules.

## 3. RESULTS AND DISCUSSION

**3.1. Design of the Overall Experimental System.** All the fabrication procedures are schematically shown in Figure 1.

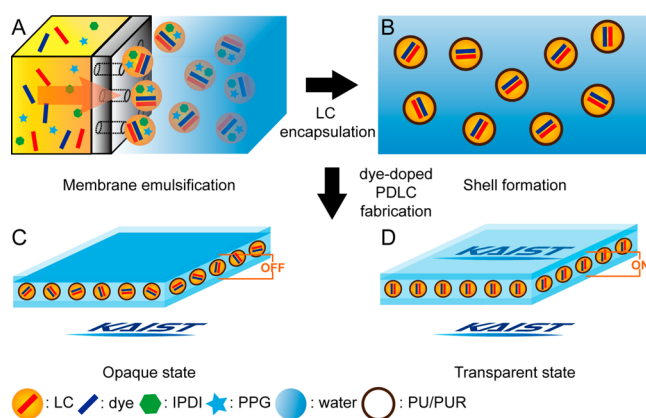


**Figure 1.** Schematic diagrams of the overall experimental system. (A) LC-containing droplet generation by the SPG membrane. (B) PU/PUR shell formation by interfacial polymerization. Electro-optical switching of dye-doped PDLC device in (C) the opaque state and (D) the transparent state by the applied electric field.

To fabricate LC-containing droplets, a hydrophobic dispersed phase (LC, dye, and monomers) was pressurized equally by nitrogen gas through a uniform pore-sized hydrophilic membrane. When the pressure reached a critical value, the LC solution overcomes the capillary pressure of the membrane pore and forms pendant drops on pores. With enough pressure to overcome the interfacial tension of each drop, the drops became sufficiently large and detached by shear force from the agitation of the surrounding water as shown in Figure 1A.<sup>30</sup> The detached droplets were stabilized by surfactants, and the polymerization began. The droplets are shown in Figure S2. The droplets had a diameter of  $4.46 \pm 0.24 \mu\text{m}$ , and the coefficient of variation was 5%. Inside the droplets, monomers reacted with each other and formed a polymer shell at the interface between the LC solution and amine-containing water as shown in Figure 1B. Finally, the fabricated capsules were applied in a dye-doped PDLC device to demonstrate control of light transmission as illustrated in panels C and D of Figure 1. The word “KAIST” was covered with the opaque dye-doped PDLC device at an off state, whereas “KAIST” can be seen when the electric field was applied to the dye-doped PDLC device.

**3.2. Mechanism of PU/PUR Capsule Formation.** To cover the LC and dye, PU/PUR was adopted as a LC-encapsulating polymer shell because of its refractive index (1.5–1.6), good mechanical property, and weatherability.<sup>31–33</sup> For the formation of a PU shell, IPDI and PPG were mixed

with a LC solution and became components of the droplets. As monomers, IPDI and PPG have an isocyanate (NCO) group and hydroxyl (OH) group, respectively (Figure 2A and reaction

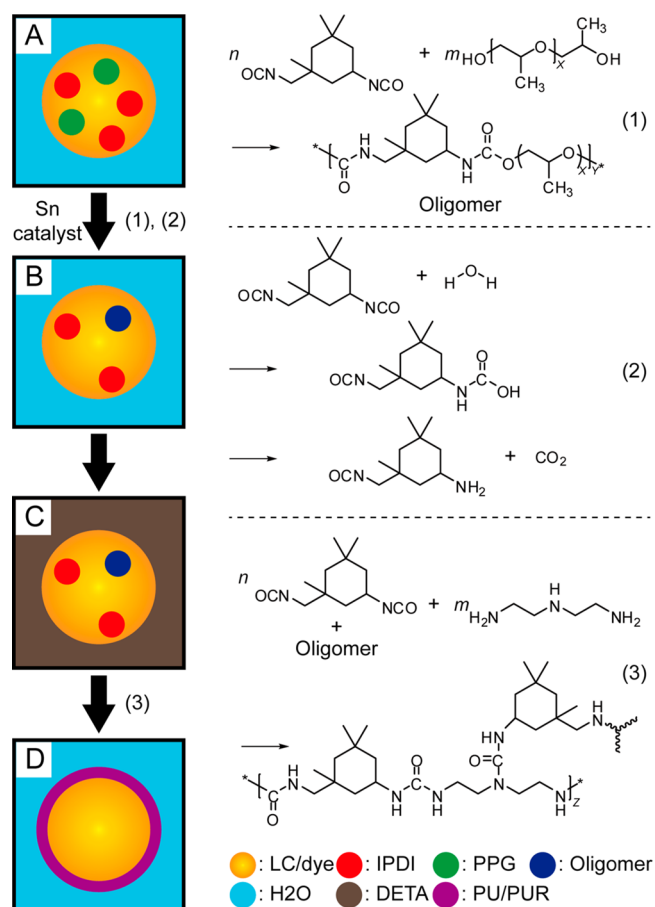


**Figure 2.** Scheme of PU/PUR shell formation. (A) IPDI, PPG, LC, and the dye-containing droplet. (B) Oligomer-synthesized droplet. (C) DETA-added droplet. (D) LC/dye-containing PU/PUR shell microcapsules. During the process, (1) urethane reaction, (2) reaction between IPDI and H<sub>2</sub>O, and (3) a urea reaction can occur.

1). Here, PPG was not only a reactant but also a nonionic surfactant that improved the stability and size distribution of the emulsion.<sup>34</sup> In an IPDI molecule, two types of NCO groups exist, a primary isocyanatomethyl and a secondary cycloaliphatic isocyanate. Between the two NCO groups, the secondary isocyanate group is more reactive than the primary isocyanatomethyl group. In comparison with the secondary isocyanate group, the primary isocyanatomethyl group is less reactive because it is shielded to a greater extent by the adjacent methyl group and  $\beta$ -carbon.<sup>33</sup>

The reaction between the NCO group and OH group did not occur at the emulsification step (Figure 2A) because of the low activity of IPDI. Hence, the produced emulsion was mixed with a Sn catalyst and heated to activate a NCO group. The catalyst made the carbonyl carbon of the NCO group electron-deficient and reactive. The activated NCO group reacted with the OH group of PPG and produced a urethane oligomer for step growth polymerization (Figure 2B and reaction 1).

In addition to reaction 1 in Figure 2, a side reaction can also occur between the NCO group and surrounding water molecules as shown in reaction 2. The NCO group forms an unstable amino acid group that dissociates into carbon dioxide

and an amine end group.<sup>35</sup> The amine group of the resulting reaction 2 participated in the following urea reaction 3 and converted to a urethane group.

After the formation of an oligomer, the remaining IPDI and oligomer reacted with DETA for further polymerization and interconnection of the oligomers by reaction 3 (Figure 2C). The DETA molecule has one reactive secondary amine in the middle and two primary amines at both ends.<sup>31</sup> The NCO group of IPDI and oligomers in a droplet reacted with the amine groups of DETA in the surrounding solution to form a urea group and cross-link the polymer chains on the surface of the droplets. After all of the reactions, LC/dye-containing PU/PUR capsules were obtained as illustrated schematically in Figure 2D.

**3.3. Characterization of Fabricated LC Capsules.** To confirm the proposed mechanism of PU/PUR shell formation, reactants and products were characterized by FT-IR (Figure 3).

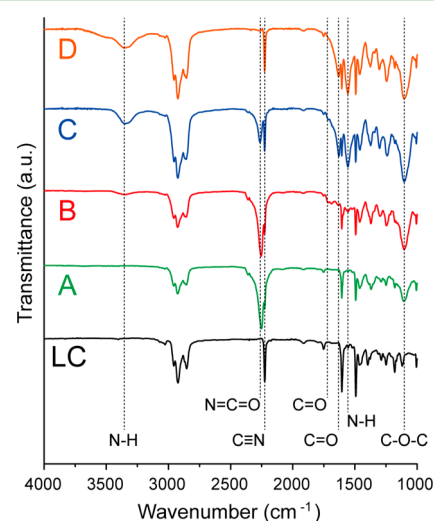


**Figure 3.** FT-IR spectra of the LC (black), (A) the IPDI/PPG/LC/dye mixture, (B) the oligomer-synthesized droplet, (C) the DETA-added droplet, and (D) the LC/dye-containing PU/PUR shell microcapsules.

In the spectra of the LC, the absorption peak located at 2225  $\text{cm}^{-1}$  was used to identify the LC. Here, the peak originated from the stretching vibration of nitrile ( $\text{C}\equiv\text{N}$ ) group, and another peak at 2950  $\text{cm}^{-1}$  was from the stretching vibration of CH in the alkyl chain. In the spectra of the dispersed phase (IPDI, PPG, and LC) (Figure 3A), the peak of the  $\text{C}\equiv\text{N}$  group appeared to be due to the LC, and other peaks were also present at 2250 and 1100  $\text{cm}^{-1}$ , which were attributed to the stretching vibration of the NCO group from the IPDI and ether ( $\text{C}-\text{O}-\text{C}$ ) group from PPG, respectively. Because of the synthesized urethane ( $-\text{NHCOO}-$ ) group, two more peaks were present at 3340  $\text{cm}^{-1}$  for the NH group and 1720  $\text{cm}^{-1}$  for the carbonyl ( $\text{C}=\text{O}$ ) group as shown in Figure 3B. The intensity of the peak of the NCO group at 2250  $\text{cm}^{-1}$  decreased sharply, and the intensity of the peak of the NH group at 3340  $\text{cm}^{-1}$  increased with the addition of DETA (Figure 3C). Furthermore, new peaks were observed at 1630 and 1560  $\text{cm}^{-1}$ , which can be ascribed to the stretching vibration of the  $\text{C}=\text{O}$  group in the urea ( $-\text{NHCONH}-$ ) group and the bending vibration of NH in the urea group. These changes and generation of peaks prove that the NCO group reacted with an added amine (DETA) and produced urea linkages. In the



spectra of the fabricated capsules (Figure 3D), we were able to observe the disappearance of the peak corresponding to the NCO group at  $2250\text{ cm}^{-1}$ , the appearance of the peak of the NH group at  $3340\text{ cm}^{-1}$ , and the peak of the  $\text{C}\equiv\text{N}$  group of LC at  $2225\text{ cm}^{-1}$ . The obtained results provide confirmation of the encapsulation of LC in PU/PUR.

**3.4. Characterization of the Morphology of LC Capsules.** The fabricated PU/PUR capsules were characterized to examine their morphology and size distribution as shown in Figure 4 and Figure S3. The capsules had a diameter

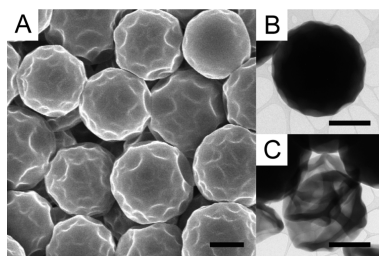


**Figure 4.** (A) SEM image of PU/PUR capsules and TEM images of the capsule (B) with LC and (C) without LC. The scale bar is  $2\text{ }\mu\text{m}$ .

of  $4.58 \pm 0.19\text{ }\mu\text{m}$  with a shell thickness of  $100\text{ nm}$  on average, and the coefficient of variation was 4%, which indicates high monodispersity.<sup>36</sup> The monodisperse capsules can prevent additional light scattering caused by interdroplet scattering of different-sized droplets. To check the core–shell structure, sliced capsules were analyzed by scanning electron microscopy (Figure S4), and transmission electron microscopy analysis was also used to observe the inside of the capsules. The fully filled dark shape (Figure 4B) represented that LC was filled in the PU/PUR capsule. The wrinkled transparent image (Figure 4C) showed a case of deflated capsules. The results confirmed a core–shell structure. Filled LC was also investigated by a polarized optical microscope.

To demonstrate the performance of the LC core, polarized light was illuminated to microcapsules as shown in Figure 5.

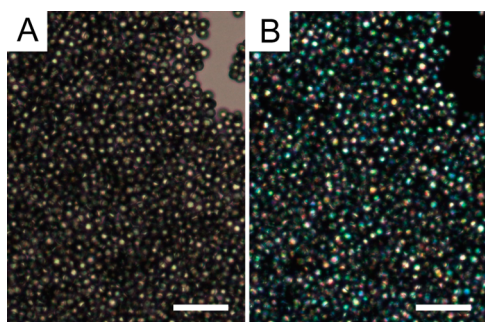


**Figure 5.** (A) Optical microscopic image of microcapsules and (B) polarization microscopic image of microcapsules. The scale bar is  $25\text{ }\mu\text{m}$ .

The LC cores showed shiny colors because of its optical anisotropy, whereas isotropic material like water was shown as black. The LC cores show aligned characteristics in Figure S5. In addition, the nematic–isotropic transition temperature was investigated (Figure S6). The original nematic–isotropic transition temperature of LC was  $95\text{ }^\circ\text{C}$ . However, the temperature of encapsulated LC with dye became  $90\text{ }^\circ\text{C}$ .

**3.5. Test of the Stability of Capsules.** Stability tests were performed to confirm the dye-doped LC holding capability of the capsules during the fabrication process (Figure S7). In panel A, the case of encapsulated LC/dye showed no peaks. In the case of cracked capsules, there were several low peaks around  $1500\text{ cm}^{-1}$ , which differed from those seen in encapsulated LC/dye tests. This result might come from the small amount of leakage of core materials. The naked droplets also showed several little peaks around  $1500\text{ cm}^{-1}$ ; in addition, this case showed LC peaks at  $1500$  and  $1600\text{ cm}^{-1}$ . This result was reasonable because the naked droplets were present in forms of emulsion, which means there were many dispersed dye-doped LCs in the water. The results show the dye-doped LC holding capability of capsules. In addition, to confirm the stability of capsules depending on time, the fabricated LC/dye–core capsules were dispersed in DI water for 0 h to 7 days (Figure S7B). The FT-IR spectra showed no peaks even after 7 days. The results showed that a PU/PUR shell successfully held the LC/dye during the fabrication process. Therefore, the proposed LC/dye encapsulation can prevent dye-related problems and enhance the electro-optical properties of the dye-doped PDLC. The capsules were also tested in various organic solvents such as acetone, ethanol, and isopropyl alcohol. In these solvents, the capsules released core materials by dissolving the capsules.

**3.6. Application and Evaluation of a Dye-Doped PDLC Device.** Using the PU/PUR capsules, we assembled a dye-doped PDLC device to demonstrate the applicability of the capsulized LC (Figure 6). The dye-doped PDLC device was

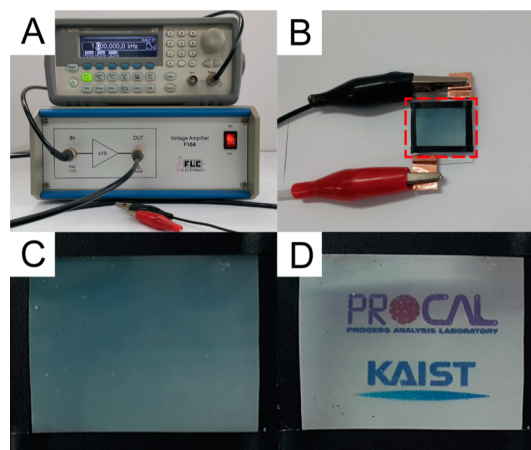


**Figure 6.** Photographs of (A) the voltage supplier and amplifier, (B) the fabricated dye-doped PDLC device, and (C) the off state (opaque) and (D) on state (transparent) of the dye-doped PDLC.

operated by supplying voltage from a function generator and a voltage amplifier (Figure 6A,B). In the absence of an electric field, LC and dye were randomly distributed. This random arrangement brought about mismatched refractive indices between the LC and polymer matrix and caused the opaque state of the dye-doped PDLC (Figure 6C). In comparison, applying an electrical field produced alignment of LC with the dye, which resulted in the refractive index matching with the polymer substrate as shown in Figure 6D.<sup>8</sup> The appearance of the previously hidden words “PROCAL” and “KAIST” indicates that a transparent state was achieved for the dye-doped PDLC.

We evaluated the electro-optical properties of dye-doped PDLC for practical application. Transmittance, CR, threshold voltage ( $V_{th}$ ), and driving voltage ( $V_{on}$ ) are typical evaluation parameters for dye-doped PDLCs.<sup>10,11,13,29,37</sup> We present the data in Figure 7 and Table 1. Parameters  $V_{th}$ ,  $V_{on}$ , and CR are

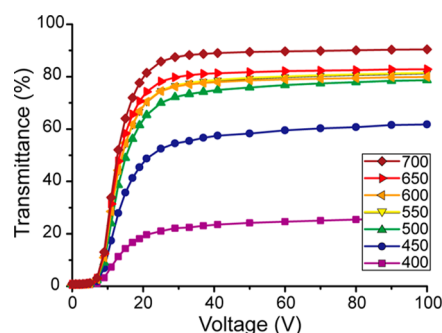


Figure 7. Applied voltage (1 kHz) dependence of the transmittance at different wavelengths.

Table 1. Electro-optical Properties of the Dye-Doped PDLC at Different Wavelengths

wavelength (nm)	$T_0$ (%)	$T_{sat}$ (%)	CR	$V_{th}$ (V)	$V_{on}$ (V)
700	0.83	90.46	109	8.1	20.9
650	0.69	82.83	120	8.1	21.3
600	0.66	79.89	121	8.2	22.4
550	0.68	81.39	120	8.3	23.6
500	0.67	78.68	117	8.6	26.4
450	0.57	61.79	108	8.7	33.5
400	0.45	26.04	58	8.4	39.9

generally defined as the voltage at 10 and 90% of the total transmittance change and the ratio between maximal transmittance ( $T_{sat}$ ) and minimal transmittance ( $T_0$ ), respectively. In Figure 7, transmittance increased with the wavelength because of the dispersed LC, which has a high transmittance at a high wavelength. As a result, the highest  $T_{sat}$  was measured in dark red light at 700 nm as 90.46. Table 1 reports the properties over a visible wavelength range. In this range, the CR was 121 at 600 nm, corresponding to orange light. This value is sufficiently high compared with those from other studies in Table 2. The enhanced CR would be a result of the synergistic effect of the dye and monodisperse capsules. On the basis of the presented data, we believe that a dye-doped PDLC device using LC/dye capsules is suitable for practical smart windows.

Table 2. Data from Other Studies

light source	dye	[dye] (wt %)	CR <sup>a</sup>
halogen laser beam, 560 nm	—	0	45–50 <sup>10</sup>
UV-vis, 600 nm	Sudan black B	0.1	117.28 <sup>29</sup>
He-Ne laser, 632.8 nm	Disperse red 1	0.015	114.6 <sup>41</sup>
white light	anthraquinone red	5	85.5 <sup>37</sup>
	Hayashibara, azo type (G-series)	0.2	~9 <sup>12</sup>
	Disperse orange 3	0.0625	105.88 <sup>13</sup>

<sup>a</sup>The CR values are the maximal values of each study.

## 4. CONCLUSION

In this work, we fabricated microcapsules to isolate LC with a dye from a polymer matrix in dye-doped PDLC to improve transmittance and to prevent problems with dye contamination. The produced LC/dye-containing PU/PUR microcapsules were monodisperse with a diameter of  $\sim 4.5 \mu\text{m}$ . A mechanism for shell formation was also proposed. Furthermore, the LC/dye holding capacity of capsules without leakage was carefully investigated. To demonstrate the capability of encapsulated LC/dye in capsules as smart windows, we fabricated a dye-doped PDLC device. The device showed a CR higher than 120 at 600 nm and a  $T_{sat}$  of 90 at 700 nm. The results for the LC/dye-core/PU/PUR-shell microcapsules and dye-doped PDLC device indicate that LC-encapsulated capsules are promising for application in flexible displays and wearable PDLCs, as well as in improved smart windows.

## ASSOCIATED CONTENT

### Supporting Information

The Supporting Information is available free of charge on the ACS Publications website at DOI: 10.1021/acsami.5b04496.

Schematic diagram of the preparation of the emulsion (Figure S1), optical microscopic image of the emulsion (Figure S2), capsule size distribution (Figure S3), SEM image of torn microcapsules (Figure S4), polarization microscopic images of rotated microcapsules (Figure S5), polarization microscopic images of LC/dye-containing capsules (Figure S6), FT-IR spectra of DI water with LC (green) and dye (red) as well as DI water in which encapsulated LC/dye (blue), cracked capsules (orange), and naked droplets (pink) were soaked and removed and DI water in which the capsules were dispersed for 0 h (green), 1 h (red), 1 day (blue), 4 days (brown), and 7 days (pink) (Figure S7) (PDF)

## AUTHOR INFORMATION

### Corresponding Author

\*E-mail: dohyun.kim@kaist.ac.kr. Fax: (+82) 42-350-3910.

### Notes

The authors declare no competing financial interest.

## ACKNOWLEDGMENTS

This research was supported by the Basic Science Research Program through the National Research Foundation of Korea (NRF) funded by the Ministry of Science, ICT & Future Planning (2014R1A5A1009799).

## REFERENCES

- Österholm, A. M.; Shen, D. E.; Kerszulis, J. A.; Bulloch, R. H.; Kuepfert, M.; Dyer, A. L.; Reynolds, J. R. Four Shades of Brown: Tuning of Electrochromic Polymer Blends Toward High-Contrast Eyewear. *ACS Appl. Mater. Interfaces* **2015**, *7*, 1413–1421.
- Kempe, M. D.; Scruggs, N. R.; Verduzco, R.; Lal, J.; Kornfield, J. A. Self-Assembled Liquid-Crystalline Gels Designed from the Bottom up. *Nat. Mater.* **2004**, *3*, 177–182.
- Wang, J.; Zhang, L.; Yu, L.; Jiao, Z.; Xie, H.; Lou, X. W. D.; Sun, X. W. A Bi-Functional Device for Self-Powered Electrochromic Window and Self-Rechargeable Transparent Battery Applications. *Nat. Commun.* **2014**, *5*, 4921.
- Runnerstrom, E. L.; Llordés, A.; Lounis, S. D.; Milliron, D. J. Nanostructured Electrochromic Smart Windows: Traditional Materials and NIR-Selective Plasmonic Nanocrystals. *Chem. Commun.* **2014**, *50*, 10555–10572.

- (5) Hosseinzadeh Khaligh, H.; Liew, K.; Han, Y.; Abukhdeir, N. M.; Goldthorpe, I. A. Silver Nanowire Transparent Electrodes for Liquid Crystal-Based Smart Windows. *Sol. Energy Mater. Sol. Cells* **2015**, *132*, 337–341.
- (6) Lampert, C. M. Large-Area Smart Glass and Integrated Photovoltaics. *Sol. Energy Mater. Sol. Cells* **2003**, *76*, 489–499.
- (7) Kumano, N.; Seki, T.; Ishii, M.; Nakamura, H.; Umemura, T.; Takeoka, Y. Multicolor Polymer-Dispersed Liquid Crystals. *Adv. Mater.* **2011**, *23*, 884–888.
- (8) West, J. L.; Ondris-Crawford, R. Characterization of Polymer Dispersed Liquid-Crystal Shutters by Ultraviolet/Visible and Infrared Absorption Spectroscopy. *J. Appl. Phys.* **1991**, *70*, 3785–3790.
- (9) Ferrari, J. A.; Dalchiele, E. A.; Frins, E. M.; Gentilini, J. A.; Perciante, C. D.; Scherschener, E. Effect of Size Polydispersity in Polymer-Dispersed Liquid-Crystal Films. *J. Appl. Phys.* **2008**, *103*, 084505.
- (10) Gao, Y.; Song, P.; Zhang, T.; Yao, W.; Ding, H.; Xiao, J.; Zhu, S.; Cao, H.; Yang, H. Effects of a Triethylamine Catalyst on Curing Time and Electro-Optical Properties of PDLC Films. *RSC Adv.* **2013**, *3*, 23533–23538.
- (11) Deshmukh, R. R.; Malik, M. K. Effect of Dichroic Dye on Phase Separation Kinetics and Electro-Optical Characteristics of Polymer Dispersed Liquid Crystals. *J. Phys. Chem. Solids* **2013**, *74*, 215–224.
- (12) Jung, J. E.; Lee, G. H.; Jang, J. E.; Hwang, K. Y.; Ahmad, F.; Muhammad, J.; Woo Lee, J.; Jeon, Y. J. Optical Enhancement of Dye-Doped PDLC by Additional Dye-LC Layer Coating. *Opt. Mater.* **2011**, *34*, 256–260.
- (13) Kumar, P.; Neeraj; Kang, S.-W.; Lee, S. H.; Raina, K. K. Analysis of Dichroic Dye-Doped Polymer-Dispersed Liquid Crystal Materials for Display Devices. *Thin Solid Films* **2011**, *520*, 457–463.
- (14) Eun Jung, J.; Lee, G. H.; Eun Jang, J.; Hwang, K. Y.; Ahmad, F.; Jamil, M.; Jin Woo, L.; Jae Jeon, Y. Optical Property Enhancement of Dye-PDLC Using Active Reflector Structure. *J. Appl. Polym. Sci.* **2012**, *124*, 873–877.
- (15) Wu, S. T.; Yang, D. K. *Fundamentals of liquid crystal devices*, 1st ed.; John Wiley and Sons: New York, 2006.
- (16) Chen, M.-Y.; Lee, J.-Y. Preparation of Dye-Doped Polymer-Dispersed Liquid Crystals Using Acrylic Monomers, and Enhancement of Contrast by Using THF Solvent as a Cleaning Agent. *J. Chin. Inst. Eng.* **2014**, *37*, 793–798.
- (17) Loiko, V. A.; Dick, V. P. Coherent Transmittance of a Polymer Dispersed Liquid Crystal Film in a Strong Field: Effect of Correlation and Polydispersity of Droplets. *Opt. Spectrosc.* **2003**, *94*, 595–599.
- (18) Gupta, J. K.; Sivakumar, S.; Caruso, F.; Abbott, N. L. Size-Dependent Ordering of Liquid Crystals Observed in Polymeric Capsules with Micrometer and Smaller Diameters. *Angew. Chem., Int. Ed.* **2009**, *48*, 1652–1655.
- (19) Lee, S. S.; Kim, B.; Kim, S. K.; Won, J. C.; Kim, Y. H.; Kim, S. H. Robust Microfluidic Encapsulation of Cholesteric Liquid Crystals Toward Photonic Ink Capsules. *Adv. Mater.* **2015**, *27*, 627–633.
- (20) Priest, C.; Quinn, A.; Postma, A.; Zelikin, A. N.; Ralston, J.; Caruso, F. Microfluidic Polymer Multilayer Adsorption on Liquid Crystal Droplets for Microcapsule Synthesis. *Lab Chip* **2008**, *8*, 2182–2187.
- (21) Khan, W.; Park, S.-Y. Configuration Change of Liquid Crystal Microdroplets Coated with a Novel Polyacrylic Acid Block Liquid Crystalline Polymer by Protein Adsorption. *Lab Chip* **2012**, *12*, 4553–4559.
- (22) Miller, D. S.; Wang, X.; Abbott, N. L. Design of Functional Materials Based on Liquid Crystalline Droplets. *Chem. Mater.* **2014**, *26*, 496–506.
- (23) Yow, H. N.; Routh, A. F. Formation of Liquid Core-Polymer Shell Microcapsules. *Soft Matter* **2006**, *2*, 940–949.
- (24) Hamlington, B. D.; Steinhaus, B.; Feng, J. J.; Link, D.; Shelley, M. J.; Shen, A. Q. Liquid Crystal Droplet Production in a Microfluidic Device. *Liq. Cryst.* **2007**, *34*, 861–870.
- (25) Lee, J.; Hwang, D. R.; Shim, S. E.; Rhym, Y.-M. Controlling Morphology of Polymer Microspheres by Shirasu Porous Glass (SPG) Membrane Emulsification and Subsequent Polymerization: From Solid to Hollow. *Macromol. Res.* **2010**, *18*, 1142–1147.
- (26) Vladislavljević, G. T.; Schubert, H. Influence of Process Parameters on Droplet Size Distribution in SPG Membrane Emulsification and Stability of Prepared Emulsion Droplets. *J. Membr. Sci.* **2003**, *225*, 15–23.
- (27) Ma, G. H.; Nagai, M.; Omi, S. Study on Preparation and Morphology of Uniform Artificial Polystyrene–Poly(methyl methacrylate) Composite Microspheres by Employing the SPG (Shirasu Porous Glass) Membrane Emulsification Technique. *J. Colloid Interface Sci.* **1999**, *214*, 264–282.
- (28) Cao, Z.; Ziener, U. A Versatile Technique to Fabricate Capsules: Miniemulsion. *Curr. Org. Chem.* **2013**, *17*, 30–38.
- (29) Ahmad, F.; Jamil, M.; Jeon, Y. J.; Woo, L. J.; Jung, J. E.; Jang, J. E. Investigation of Nonionic Diazo Dye-Doped Polymer Dispersed Liquid Crystal Film. *Bull. Mater. Sci.* **2012**, *35*, 221–231.
- (30) Geerken, M. J.; Lammertink, R. G. H.; Wessling, M. Interfacial Aspects of Water Drop Formation at Micro-Engineered Orifices. *J. Colloid Interface Sci.* **2007**, *312*, 460–469.
- (31) Jabbari, E.; Khakpour, M. Morphology of and Release Behavior from Porous Polyurethane Microspheres. *Biomaterials* **2000**, *21*, 2073–2079.
- (32) Mark, J. E. *Polymer Data Handbook*, 1st ed.; Oxford University Press: Oxford, U.K., 1999.
- (33) Lomölder, R.; Plogmann, F.; Speier, P. Selectivity of Isophorone Diisocyanate in the Urethane Reaction Influence of Temperature, Catalysis, and Reaction Partners. *J. Coat. Technol.* **1997**, *69*, 51–57.
- (34) Lu, S.; Xing, J.; Zhang, Z.; Jia, G. Preparation and Characterization of Polyurea/Polyurethane Double-Shell Microcapsules Containing Butyl Stearate through Interfacial Polymerization. *J. Appl. Polym. Sci.* **2011**, *121*, 3377–3383.
- (35) Xu, J.; Han, H.; Zhang, L.; Zhu, X.; Jiang, X.; Kong, X. Z. Preparation of Highly Uniform and Crosslinked Polyurea Microspheres through Precipitation Copolymerization and Their Property and Structure Characterization. *RSC Adv.* **2014**, *4*, 32134–32141.
- (36) Tang, L.; Fan, T. M.; Borst, L. B.; Cheng, J. Synthesis and Biological Response of Size-Specific, Monodisperse Drug-Silica Nanoconjugates. *ACS Nano* **2012**, *6*, 3954–3966.
- (37) Yang, K.-J.; Lee, S.-C.; Choi, B.-D. Dye-Doped Polymer Dispersed Liquid Crystal Films for Flexible Displays. *Jpn. J. Appl. Phys.* **2010**, *49*, 05EA05.